Journal of Electronic Research and Application, 2026, Volume 10, Issue 5
http://ojs.bbwpublisher.com/index.php/JERA
Online ISSN: 2208-3510
Print ISSN: 2208-3502

Nondestructive Detection of Moldy In-shell Walnuts Using Visible Hyperspectral Imaging Combined with 1D-CNN

Ming Liu*

School of Information, Yunnan Normal University, Kunming 650500, China

Corresponding author: Ming Liu, 2324100031@ynnu.deu.cn

Abstract: To achieve rapid and nondestructive detection of moldy in-shell walnuts, this study proposes a walnut mold detection method based on visible hyperspectral imaging combined with a one-dimensional convolutional neural network (1D-CNN). Complete in-shell walnuts were used as the research objects, and hyperspectral data of normal and moldy walnuts were collected in the wavelength range of 400–900 nm. The raw hyperspectral images were processed through reflectance correction, region of interest extraction, average spectral curve construction, Savitzky-Golay (SG) smoothing, and standard normal variate (SNV) transformation. These preprocessing steps were used to reduce the influence of system noise, background interference, and scattering effects caused by differences in walnut shell morphology. On this basis, the processed spectral data were used as the input of a 1D-CNN model to classify normal and moldy walnuts. The experimental results showed that the proposed model achieved an Accuracy of 0.867, Precision of 0.923, Recall of 0.800, and F1-score of 0.857 on the test set. The results indicate that visible hyperspectral imaging can capture spectral variations caused by mold development in in-shell walnuts, and the combination of visible hyperspectral imaging and 1D-CNN can effectively identify moldy walnuts. This study provides a feasible method for nondestructive quality detection of walnuts.

Keywords: Hyperspectral imaging; Walnut mold; Nondestructive detection; 1D-CNN; Visible spectrum

Online publication: Jun 29, 2026

1. Introduction

Walnuts are an important nut product with high economic and nutritional value. They are rich in fat, protein, unsaturated fatty acids, and various micronutrients. However, during postharvest storage, transportation, and circulation, walnuts are susceptible to mold growth under unfavorable environmental conditions such as high humidity, improper temperature, and long storage time. Mold development not only affects walnut appearance and edible quality but may also lead to the production of harmful metabolites, posing potential

risks to food safety. Therefore, rapid and accurate detection of moldy walnuts is of great significance for quality control and food safety assurance [1].

At present, mold detection in walnuts mainly relies on manual inspection, physicochemical analysis, and microbial culture. Manual inspection is simple but highly subjective, and its accuracy depends heavily on the experience of inspectors. Physicochemical and microbial detection methods can provide reliable results, but they usually require complex sample preparation, long detection time, and destructive operations. These limitations make them difficult to apply to rapid screening and online detection of in-shell walnuts. Therefore, it is necessary to develop a nondestructive, efficient, and relatively accurate detection method for walnut mold identification [2].

Hyperspectral imaging technology integrates imaging and spectroscopy, enabling the simultaneous acquisition of spatial and spectral information from samples. Compared with ordinary image detection, hyperspectral imaging can provide continuous spectral responses that reflect material composition and surface characteristics. In the field of agricultural product quality detection, hyperspectral imaging has shown strong potential for identifying defects, diseases, and quality changes [3]. In recent years, hyperspectral imaging has been widely used in food safety inspection, agricultural product quality evaluation, and nondestructive detection because of its rich spectral information and imaging capability [4]. For in-shell walnuts, mold development may cause changes in shell surface color, tissue structure, and reflectance characteristics. These changes may be reflected in the visible spectral range, making visible hyperspectral imaging a potential tool for mold detection [5].

In addition, deep learning methods have been widely used in classification and pattern recognition tasks because of their strong feature learning ability [6]. Convolutional neural networks (CNNs) can automatically extract effective features from input data and reduce the dependence on manual feature design. Since hyperspectral data can be regarded as continuous spectral sequences along the wavelength dimension, a one-dimensional convolutional neural network (1D-CNN) is suitable for learning local spectral variation patterns between adjacent bands [7]. Compared with traditional classification methods, 1D-CNN can better explore the spectral continuity and local correlation of hyperspectral data.

Based on this, this study used complete in-shell walnuts as the research objects and collected visible hyperspectral data in the range of 400–900 nm. After reflectance correction, ROI extraction, and spectral preprocessing, a 1D-CNN model was constructed to identify normal and moldy walnuts. The purpose of this study is to explore the feasibility of visible hyperspectral imaging combined with 1D-CNN for nondestructive detection of moldy in-shell walnuts [8].

2. Materials and methods

2.1. Walnut samples and hyperspectral data acquisition

A total of 200 complete in-shell walnut samples were collected in this study, including 100 normal walnuts and 100 moldy walnuts. The normal walnuts were selected from samples with intact appearance and no obvious odor, while the moldy walnuts were obtained from samples that developed mold during natural storage (**Figure 1**). Before data acquisition, all samples were manually screened and labeled according to their actual mold condition. Samples with severe mechanical damage or defects unrelated to mold were excluded to reduce interference in subsequent modeling [9].

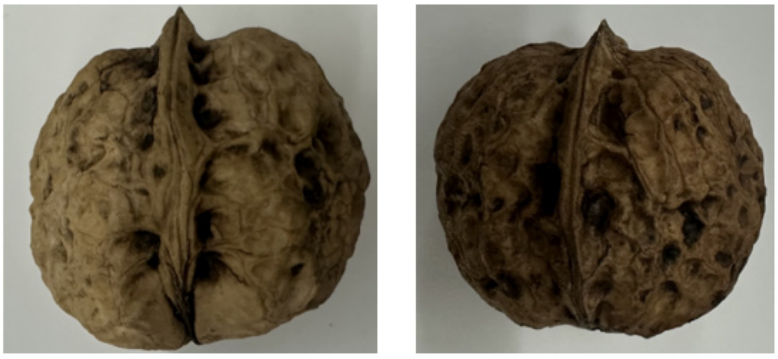

Figure 1. Appearance comparison of walnut samples with different mold conditions: (a) Normal walnut; (b) Moldy walnut.

A line-scan visible hyperspectral imaging system was used to acquire hyperspectral data from the walnut samples. The spectral range of the system was 400–900 nm, and the sampling interval was 5 nm, resulting in 101 continuous spectral bands. The system mainly consisted of an imaging spectrometer, an industrial camera, a uniform illumination system (**Figure 2**), a motorized scanning platform, and data acquisition software [10].

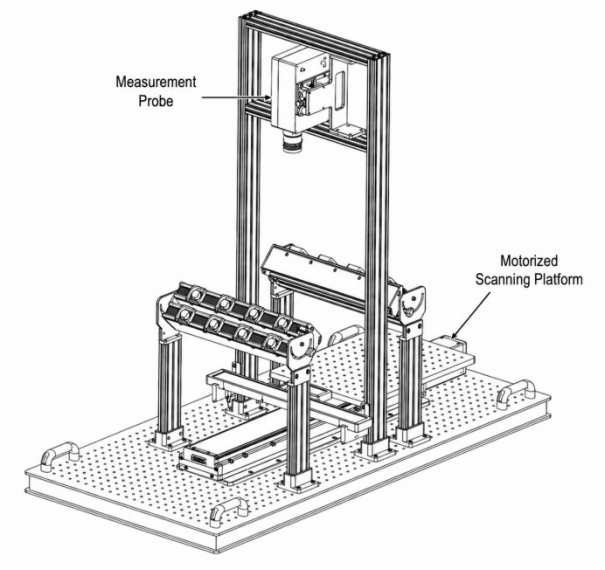

Figure 2. Visible hyperspectral imaging system.

During image acquisition, each walnut sample was placed on the motorized scanning platform, and the scanning speed, exposure time, and illumination conditions were kept consistent. The line-scan imaging system acquired the sample image line by line through relative motion between the sample and the imaging system. Finally, a three-dimensional hyperspectral data cube containing two spatial dimensions and one spectral dimension was obtained for each sample [11].

Before formal data acquisition, dark-field correction and white-reference correction were performed

to reduce the influence of camera dark current, system noise, and uneven illumination. The reflectance correction formula is expressed as follows:

$$R = \frac{I - D}{W - D}$$

where R is the corrected reflectance image, I is the original hyperspectral image, D is the dark-field image, and W is the white-reference image.

After reflectance correction, the spectral data of different samples became more comparable under the same wavelength conditions.

2.2. ROI extraction and spectral preprocessing

The original hyperspectral images contained both walnut regions and background regions. Since the background pixels do not contribute to mold detection and may introduce interference, it was necessary to extract the walnut region before spectral analysis. According to preliminary observations, the walnut samples and background showed a clear gray-level difference at the 650 nm band. Therefore, the image at 650 nm was selected as the reference image for threshold segmentation [12].

After threshold segmentation, the walnut region was retained as the region of interest (ROI), and the background pixels were removed. The ROI mask was then applied to all spectral bands in the range of 400–900 nm. For each wavelength, the reflectance values of all valid pixels within the ROI were averaged to construct the average spectral curve of each sample. This operation reduced the influence of local surface noise and obtained a stable spectral representation for each walnut sample.

The average reflectance at wavelength λ is calculated as follows:

$$\overline{R_\lambda} = \frac{1}{N}\sum_{i=1}^{N} R_{i\lambda}$$

where N **is** the number of valid pixels within the ROI, and $R_{i\lambda}$ represents the reflectance value of the i-th pixel at wavelength λ.

To further improve the quality of spectral data, SG smoothing and SNV transformation were applied to the average spectral curves. SG smoothing was used to reduce random noise while preserving the overall shape and variation trend of the spectral curves [13]. SNV transformation was used to reduce scattering effects caused by differences in shell roughness, sample morphology, and illumination angle [14]. These preprocessing steps helped improve the comparability of spectra between different walnut samples (**Figure 3**).

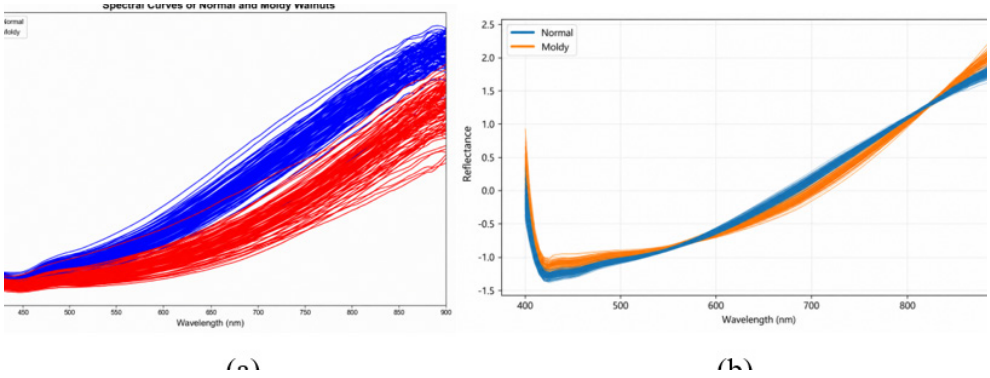

Figure 3. Comparison of walnut spectra before and after preprocessing: (a) Raw spectra; (b) Spectra after SG+SNV preprocessing.

After preprocessing, each walnut sample was represented by a one-dimensional spectral vector with 101 bands. These spectral vectors were used as the input data for subsequent 1D-CNN modeling.

2.3. Construction of the 1D-CNN model

A one-dimensional convolutional neural network was constructed to classify normal and moldy walnuts. Each sample was represented by a spectral vector with a length of 101, corresponding to the continuous spectral information in the range of 400–900 nm. Spectral data can be effectively modeled as one-dimensional sequential data, and deep learning methods have shown potential in extracting useful features from such spectral inputs [15,16].

The 1D-CNN model mainly consisted of three convolutional layers, pooling layers, a fully connected layer, and an output layer. The convolutional layers were used to extract local spectral features from adjacent wavelength bands. The kernel sizes of the three convolutional layers were set to 7, 5, and 3, respectively, and the numbers of convolution kernels were 32, 64, and 128. Each convolutional layer was followed by a ReLU activation function to introduce nonlinear mapping ability [17]. Max pooling was used after convolution to reduce feature dimensions and suppress noise interference (**Figure 4**).

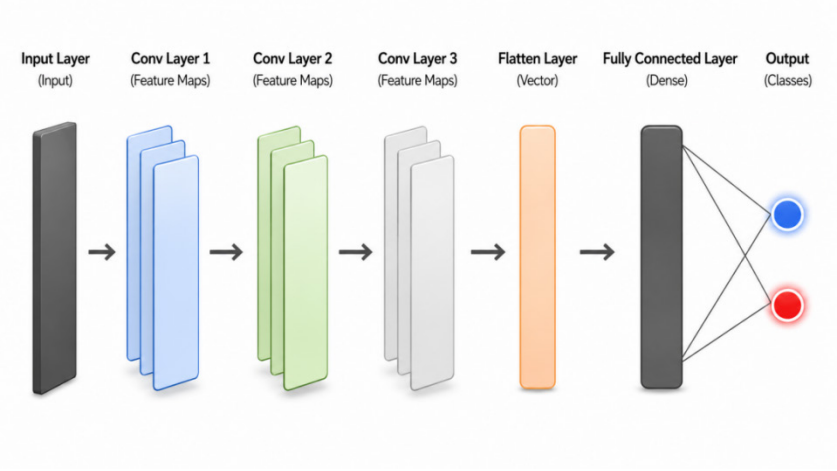

Figure 4. Structure of the 1D-CNN model for walnut mold detection.

After feature extraction, the output feature maps were flattened and passed through the fully connected layer. The output layer used the Softmax function to obtain the classification probabilities of normal and moldy walnuts. The category with the higher probability was taken as the final prediction result.

The dataset was divided into training, validation, and test sets at a ratio of 70%:15%:15%. The training set was used for model parameter learning, the validation set was used for parameter adjustment and overfitting control, and the test set was used to evaluate the final classification performance. The Adam optimizer was used to update model parameters, with a learning rate of 0.001, a batch size of 32, and a maximum of 100 training epochs [18].

The cross-entropy loss function is expressed as follows:

$$L = -\frac{1}{N}\sum_{i=1}^{N}\sum_{c=1}^{c} y_{ic}\log\left(p_{ic}\right)$$

where (y_{ic}) epresents the true label of the i-th sample for class (c), and (p_{ic}) represents the predicted probability output by the model.

3. Results and analysis

3.1. Model classification performance

The constructed 1D-CNN model was evaluated on the test set. The evaluation metrics included Accuracy, Precision, Recall, and F1-score. Accuracy reflects the overall proportion of correctly classified samples. Precision reflects the reliability of samples predicted as moldy, while Recall reflects the ability of the model to identify actual moldy samples. F1-score provides a comprehensive evaluation by considering both Precision and Recall.

The experimental results showed that the model achieved an Accuracy of 0.867, Precision of 0.923, Recall of 0.800, and F1-score of 0.857 on the test set (**Table 1**).

Table 1. Classification performance of the 1D-CNN model on the test set

Model	Accuracy	Precision	Recall	F1-score
1D-CNN	0.867	0.923	0.800	0.857

The results indicate that the 1D-CNN model constructed using visible hyperspectral data in the range of 400–900 nm can effectively distinguish normal walnuts from moldy walnuts. The high Precision value indicates that most samples predicted as moldy were correctly classified. However, the Recall value was slightly lower, suggesting that some moldy walnuts were not successfully identified.

3.2. Confusion matrix analysis

The confusion matrix was used to further analyze the classification performance of the model on different categories. The results showed that 26 out of 30 test samples were correctly classified. Among them, 14 normal walnuts and 12 moldy walnuts were correctly identified.

A total of 4 samples were misclassified, including 1 normal walnut misclassified as moldy and 3 moldy walnuts misclassified as normal (**Figure 5**).

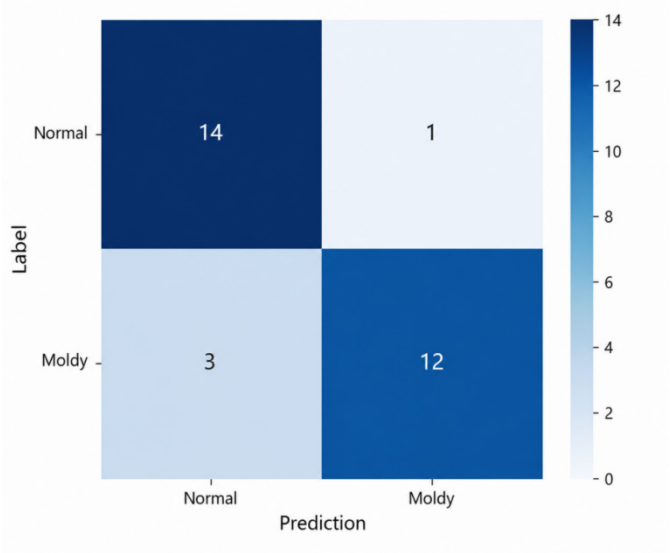

Figure 5. Confusion matrix of the 1D-CNN model.

The confusion matrix results indicate that the model had relatively stable recognition performance for normal walnut samples. However, missed detection still occurred for some moldy samples. This may be because some mildly moldy walnuts had weak spectral differences in the visible wavelength range, making them difficult to distinguish from normal walnuts. From the perspective of practical application, reducing missed detection of moldy samples is particularly important, and further optimization is needed in future work.

3.3. Discussion

The experimental results show that visible hyperspectral data can reflect, to some extent, the spectral variations caused by mold development in walnuts. The continuous spectral information in the range of 400–900 nm preserves the reflectance characteristics of walnut shells. When mold occurs, changes in shell surface color, tissue state, and local structure may affect the reflectance response at different wavelengths. Therefore, the spectral sequence contains useful information for distinguishing normal and moldy walnuts.

The use of SG smoothing and SNV transformation also contributed to improving the stability of the spectral data. SG smoothing reduced random fluctuations in the spectral curves, while SNV transformation weakened spectral differences caused by scattering effects and sample morphology. This made the spectral curves more suitable for subsequent model learning.

The 1D-CNN model was able to automatically extract local variation features from the spectral sequence. Compared with manual feature extraction, 1D-CNN can learn more flexible spectral patterns and capture relationships between adjacent bands. This is beneficial for identifying subtle spectral differences caused by mold development.

However, there are still some limitations in this study. First, the number of samples was relatively limited, which may affect the generalization ability of the model. Second, the detection was based only on the visible wavelength range of 400–900 nm. For some mildly moldy samples, the spectral changes in the visible range may not be sufficiently obvious. Third, the roughness, texture, shape, and local shadow of walnut shells may introduce additional spectral variation unrelated to mold. These factors may lead to misclassification.

In future research, the sample size can be further expanded, and samples with different mold degrees can be included to improve model robustness. In addition, near-infrared spectral information or improved deep learning structures can be introduced to further enhance the detection accuracy and stability of the model.

4. Conclusion

This study proposed a nondestructive detection method for moldy in-shell walnuts based on visible hyperspectral imaging combined with 1D-CNN. Hyperspectral data of walnut samples in the range of 400–900 nm were collected, and reflectance correction, ROI extraction, average spectral curve construction, and SG+SNV preprocessing were performed to obtain spectral data for model training and testing. On this basis, a 1D-CNN classification model was constructed to identify normal and moldy walnuts. The experimental results showed that the 1D-CNN model achieved an Accuracy of 0.867, Precision of 0.923, Recall of 0.800, and F1-score of 0.857 on the test set, indicating that visible hyperspectral imaging combined with 1D-CNN can effectively identify moldy in-shell walnuts. Overall, the proposed method can realize nondestructive identification of walnut mold status and has potential application value in walnut quality screening. However,

the model still showed missed detections for some moldy samples. Future work will focus on expanding the sample size, improving the model structure, and introducing richer spectral information to further improve the accuracy and stability of walnut mold detection.

Disclosure statement

The author declares no conflict of interest.

References

[1] Gürses M, 2006, Mycoflora and Aflatoxin Content of Hazelnuts, Walnuts, Peanuts, Almonds and Roasted Chickpeas (LEBLEBI) Sold in Turkey. International Journal of Food Properties, 9(3): 395–399.

[2] Xu J, Xu D, Bai X, et al., 2022, Non-Destructive Detection of Moldy Walnuts based on Hyperspectral Imaging Technology. Molecules, 27(20): 6776.

[3] Huang H, Liu L, Ngadi M, 2014, Recent Developments in Hyperspectral Imaging for Assessment of Food Quality and Safety. Sensors, 14(4): 7248–7276.

[4] Feng Y, Sun D, 2012, Application of Hyperspectral Imaging in Food Safety Inspection and Control: A Review. Critical Reviews In Food Science and Nutrition, 52(11): 1039–1058.

[5] Liu Y, Pu H, Sun D, 2017, Hyperspectral Imaging Technique for Evaluating Food Quality and Safety during Various Processes: A Review of Recent Applications. Trends in Food Science & Technology, 2017(69): 25–35.

[6] LeCun Y, Bengio Y, Hinton G, 2015, Deep Learning. Nature, 521(7553): 436–444.

[7] Chen X, Cheng G, Liu S, et al., 2022, Probing 1D Convolutional Neural Network Adapted to Near-Infrared Spectroscopy for Efficient Classification of Mixed Fish. Spectrochimica Acta Part A: Molecular and Biomolecular Spectroscopy, 2022(279): 121350.

[8] Kheiralipour K, Sajadipour F, Nadimi M, 2025, A Review of Nut Quality Assessment using Hyperspectral Imaging Technique. Journal of Food Composition and Analysis, 2025: 108184.

[9] Naeem I, Ismail A, Rehman A, et al., 2022, Prevalence of Aflatoxins in Selected Dry Fruits, Impact of Storage Conditions on Contamination Levels and Associated Health Risks on Pakistani Consumers. International Journal of Environmental Research and Public Health, 19(6): 3404.

[10] Elmasry G, Kamruzzaman M, Sun D, et al., 2012, Principles and Applications of Hyperspectral Imaging in Quality Evaluation of Agro-Food Products: A Review. Critical Reviews in Food Science and Nutrition, 52(11): 999–1023.

[11] Burger J, Geladi P, 2005, Hyperspectral NIR Image Regression Part I: Calibration and Correction. Journal of Chemometrics: A Journal of the Chemometrics Society, 19(5–7): 355–363.

[12] Pu Y, Feng Y, Sun D, 2015, Recent Progress of Hyperspectral Imaging on Quality and Safety Inspection of Fruits and Vegetables: A Review. Comprehensive Reviews in Food Science and Food Safety, 14(2): 176–188.

[13] Savitzky A, Golay M, 1964, Smoothing and Differentiation of Data by Simplified Least Squares Procedures. Analytical Chemistry, 36(8): 1627–1639.

[14] Barnes R, Dhanoa M, Lister S, 1989, Standard Normal Variate Transformation and De-Trending of Near-Infrared Diffuse Reflectance Spectra. Applied Spectroscopy, 43(5): 772–777.

[15] Mishra P, Passos D, Marini F, et al., 2022, Deep Learning for Near-Infrared Spectral Data Modelling: Hypes and Benefits. TrAC Trends in Analytical Chemistry, 2022(157): 116804.

[16] Malek S, Melgani F, Bazi Y, 2018, One-Dimensional Convolutional Neural Networks for Spectroscopic Signal

Regression. Journal of Chemometrics, 32(5): e2977.

[17] He K, Zhang X, Ren S, et al., 2015, Delving Deep into Rectifiers: Surpassing Human-Level Performance on Imagenet Classification, Proceedings of the IEEE International Conference on Computer Vision, 1026–1034.

[18] Kingma D, Ba J. Adam, 2014, A Method for Stochastic Optimization, arXiv preprint arXiv:1412.6980.